Inorganic Chemistry

ARTICLE

pubs.acs.org/IC

Mechanistic Studies on the Reactions of Cyanide with a Water-Soluble Fe(III) Porphyrin and Their Effect on the Binding of NO

Maria Oszajca,[†,‡] Alicja Franke,[†] Małgorzata Brindell,[‡] Grażyna Stochel,[*,‡] and Rudi van Eldik[*,†]

[†]Inorganic Chemistry, Department of Chemistry and Pharmacy, University of Erlangen-Nürnberg, Egerlandstrasse 1, 91058 Erlangen, Germany

[‡]Faculty of Chemistry, Jagiellonian University, Ingardena 3, 30-060 Kraków, Poland

ABSTRACT: The reaction of the water-soluble Fe^{III}(TMPS) porphyrin with CN^- in basic solution leads to the stepwise formation of Fe^{III}(TMPS)(CN)(H_2O) and Fe^{III}(TMPS)-$(CN)_2$. The kinetics of the reaction of CN^- with Fe^{III}(TMPS)-(CN)(H_2O) was studied as a function of temperature and pressure. The positive value of the activation volume for the formation of Fe^{III}(TMPS)$(CN)_2$ is consistent with the operation of a dissociatively activated mechanism and confirms the six-coordinate nature of the monocyano complex. A good agreement between the rate constants at pH 8 and 9 for the formation of the dicyano complex implies the presence of water in the axial position trans to coordinated cyanide in the monocyano complex and eliminates the existence of Fe^{III}(TMPS)(CN)(OH) under the selected reaction conditions. Both Fe^{III}(TMPS)-(CN)(H_2O) and Fe^{III}(TMPS)$(CN)_2$ bind nitric oxide (NO) to form the same nitrosyl complex, namely, Fe^{II}(TMPS)(CN)-(NO^+). Kinetic studies indicate that nitrosylation of Fe^{III}(TMPS)$(CN)_2$ follows a limiting dissociative mechanism that is supported by the independence of the observed rate constant on [NO] at an appropriately high excess of NO, and the positive values of both the activation parameters $\Delta S^{\ddagger}$ and $\Delta V^{\ddagger}$ found for the reaction under such conditions. The relatively small first-order rate constant for NO binding, namely, $(1.54 \pm 0.01) \times 10^{-2}$ s^{-1}, correlates with the rate constant for CN^- release from the Fe^{III}(TMPS)$(CN)_2$ complex, namely, $(1.3 \pm 0.2) \times 10^{-2}$ s^{-1} at 20 °C, and supports the proposed nitrosylation mechanism.

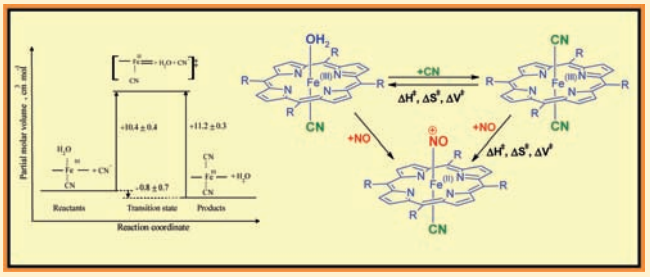

INTRODUCTION

Nitric oxide (NO) was proclaimed the molecule of the year by *Science* in 1992 since the important biological significance of this messenger molecule was confirmed by many extensive studies on the role of NO in mammalian biology.[1] Since the physiological and pathophysiological role of NO is often related to its coordination to metal centers, in particular iron, the interaction of hemoproteins and different modified, water-soluble iron porphyrin complexes with NO has been intensively studied over the past years.[2−6] The dynamics of the formation and stability of nitrosyl porphyrin complexes depends on various factors, for instance, the nature and overall charge on the porphyrin, oxidation state of the iron center, spin reorganization, lability of the metal center, and the nature of the axial ligands.[7] In addition to the character of the prosthetic group, numerous other factors connected with the protein structure have a large influence on the reversible binding of NO to the iron center. Thus, a comparison of the results obtained from studies on the nitrosylation of iron porphyrins with those obtained from studies on the binding of NO to hemoproteins enabled the elucidation of the role of the protein structure on the properties of the heme coordination center and the regulation of NO binding. Because of the many factors that govern NO coordination to iron hemes and NO dissociation from nitrosyl complexes, the elucidation of the mechanism of NO interaction with iron porphyrins is still far from complete and requires more detailed studies.

Systematic studies on the interaction of NO with $[Fe^{III}(TMPS)]^{3-}$, [*meso*-tetrakis(2,4,6-trimethyl-3-sulfonatophenyl)porphinato]-iron(III), a water-soluble synthetic model iron porphyrin, indicated that this complex is a reasonable model for the ferriheme protein, particularly met-myoglobin.[2] The mechanism of reversible binding of NO to Fe^{III}(TMPS) was shown to depend strongly on the pH of the solution.[6] At low pH where Fe^{III}(TMPS) exists as a six-coordinate diaqua-ligated species $[Fe^{III}$(TMPS)-$(H_2O)_2]^{3-}$, coordination of NO occurs via a dissociatively activated mechanism and is controlled by the lability of the metal center.[2] An opposite, associatively activated mechanism was observed for the binding of NO to the five-coordinate monohydroxo species $[Fe^{III}(TMPS)(OH)]^{4-}$ at high pH. On the basis of detailed mechanistic studies, it was proposed that formation of Fe^{II}(TMPS)(OH)(NO^+) is controlled by Fe^{III}-NO bond formation and spin reorganization connected with this process.[6]

Mechanistic studies on the binding of NO to Fe^{III}(TMPS)-(OH)(MeIm) in an ionic liquid revealed that coordination of methylimidazole (MeIm) to the monohydroxo porphyrin species

Received: November 22, 2010
Published: March 23, 2011

dx.doi.org/10.1021/ic1023345 | *Inorg. Chem.* 2011, 50, 3413–3424

led to a changeover in mechanism for the formation of $Fe^{II}(TMPS)(OH)(NO^+)$ from an associatively activated mode for $Fe^{III}(TMPS)(OH)$ to a dissociatively activated mode for $Fe^{III}(TMPS)(OH)(MeIm)$.[8] In a preliminary study, we also attempted to generate the mono(methylimidazole) $Fe^{III}(TMPS)$ derivative in aqueous solution. However, formation of only the bis(methylimidazole) complex $Fe^{III}(TMPS)(MeIm)_2$ was observed over a wide pH range (pH = 5−13). The binding of NO to the bis(methylimidazole) porphyrin complex revealed only formation of $Fe^{II}(TMPS)(OH)(NO^+)$ from $Fe^{III}(TMPS)(OH)$ existing in equilibrium with $Fe^{III}(TMPS)(MeIm)_2$. Subsequent reductive nitrosylation, which occurs much faster in the presence of MeIm, rendered it impossible to monitor the binding of NO to $Fe^{III}(TMPS)(MeIm)_2$.

It follows from the above discussion that the number and electronic nature of the axial ligands in synthetic model ferric porphyrins can regulate the dynamics of NO binding as well as the stability and reactivity of the nitrosyl adducts. Therefore, to investigate the influence of the nature of the axial ligand on the reactivity of iron(III) porphyrins with NO, we selected the cyanide ligand which behaves as a strong σ donor and π acceptor. The cyanide ion has been extensively used in the study of the properties of iron porphyrins, hemes, and hemoproteins,[9−12] as well as in many modeling studies on simple iron complexes.[13] Although both ferric and ferrous iron porphyrins can interact with cyanide, the affinity of cyanide for the iron(III) heme center is much higher. The binding of cyanide to the ferric heme center leads to the formation of low-spin dicyano $Fe^{III}(Por)(CN)_2$ or mixed-ligand $Fe^{III}(Por)(CN)(L)$ complexes.[9,10] Cyanide for example binds to the heme a_3 oxygen site of cytochrome *c* oxidase and strongly inhibits the catalytic activity of the enzyme, and as a result studies in search for methods to treat cyanide poisoning have received significant attention.[14]

In the present study we chose the water-soluble porphyrin $Fe^{III}(TMPS)$ and by addition of appropriate amounts of sodium cyanide under selected pH conditions generated the six-coordinate $Fe^{III}(TMPS)(CN)(H_2O)$ and $Fe^{III}(TMPS)(CN)_2$ species. Detailed kinetic studies on the reactions of the cyanide derivatives of $Fe^{III}(TMPS)$ with NO were performed. To obtain a better understanding of the mechanism of NO coordination to cyano porphyrin complexes, we supplemented our study with kinetic measurements on the formation of the mono- and dicyano $Fe^{III}(TMPS)$ complexes. All measurements were performed at two selected pH values (namely, 8 and 9), for which the $Fe^{III}(TMPS)$ complex mainly exists as $Fe^{III}(TMPS)(OH)$ since the pK_a of $Fe^{III}(TMPS)(H_2O)_2$ is 6.9. Comparison of the kinetic data from two different pH values helped us to identify the nature of the monocyano species which participated in the observed reactions. Furthermore, the selected pH conditions enabled us to follow the formation of the monocyano porphyrin complex and the subsequent formation of the dicyano complex.

EXPERIMENTAL SECTION

Materials. All chemicals used in this study were of analytical reagent grade. NO gas was purchased from Praxair Deutschland GmbH & Co. KG, Bopfingen (3.0) and bubbled through concentrated KOH solution to remove higher nitrogen oxides (N_2O_3, NO_2), then passed through an Ascrite II column (NaOH on silica gel, Sigma Aldrich) and a phosphorus pentoxide column. The iron(III) porphyrin, [*meso*-tetrakis(2,4,6-trimethyl-3-sulfonatophenyl)porphinato]-iron(III) hydroxide (tetrasodium salt), was purchased from Frontier Scientific, Inc. Utah, U.S.A. Sodium cyanide was purchased from Aldrich Chemical Co., Inc. and used as source for cyanide throughout the study.

Solution Preparation. Samples of $Fe^{III}(TMPS)(OH)$ were prepared at pH 8 and 9 using TAPS (>99%, ROTH) and CHES (>99%, Sigma) buffer solutions (0.05 M), respectively. The ionic strength of the solutions was adjusted with $NaNO_3$ to 0.15 M. Deionized water was used for the preparation of all solutions. Since experiments with NO required an inert atmosphere, all solutions were deoxygenated by argon and handled using gastight syringes. Appropriate concentrations of NO (0.2−1.8 mM) were prepared by mixing a saturated solution of NO (1.8 mM) with a deoxygenated buffer solution under inert atmosphere. Cyanide derivatives of $Fe^{III}(TMPS)$ were obtained by addition of an appropriate excess of NaCN.

Measurements. Ambient pressure stopped-flow measurements were performed on an SX 18.MV Applied Photophysics apparatus equipped with a thermostat (±0.1 °C). In a typical experiment, buffer solutions (deoxygenated if required) of the porphyrin complex were rapidly mixed with appropriate concentrated substrate solutions (NO or NaCN) in the ratio 1:1. All reactions with NO were initiated using pre-equilibrated solutions of $Fe^{III}(TMPS)(OH)$ with cyanide. All kinetic measurements were performed under pseudo first-order conditions, that is, by using at least a 10-fold excess of NO or NaCN (representing the total cyanide concentration in the solution) over the porphyrin concentration. Reported rate constants are mean values of at least 10 kinetic runs. Time-resolved spectra were recorded with the use of the stopped-flow apparatus described above, equipped with a J&M TIDAS diode-array detector. High pressure stopped-flow experiments were performed in the pressure range of 10 to 130 MPa on a custom built apparatus.[15] OLIS KINFIT software (Bogart, GA, 1989) was used for the analysis of kinetic traces. Ambient pressure UV−vis spectra were recorded on a Shimadzu UV−2101PC spectrophotometer equipped with a thermostatted cell compartment (CPS-260). UV−vis spectra under high pressure conditions (up to 150 MPa) were recorded in a quartz pill-box cell on the spectrophotometer described above including a custom built high pressure cell.[16]

RESULTS AND DISCUSSION

UV−vis Spectral Data for the Reaction of $Fe^{III}(TMPS)(OH)$ with Cyanide. The UV−vis spectrum of $Fe^{III}(TMPS)(OH)$ exhibits a Soret band maximum at 416 nm. After addition of an excess of sodium cyanide to the $Fe^{III}(TMPS)(OH)$ complex, two subsequent reactions were observed. The first fast reaction leadingto formation of the monocyano species revealed an absorbance increase in the Soret band at 416 nm and the appearance of a new Q-band at 550 nm (Figure 1a). The second reaction connected with conversion of the monocyano to the dicyano complex occurred on a much slower time scale and resulted in the spectral changes presented in Figure 1b. The decrease in the Soret band at 416 nm was accompanied by a simultaneous appearance of a new Soret band at 427 nm and an increase in absorbance at 600 nm.

Kinetic and Thermodynamic Studies on the Reaction of CN^- with $Fe^{III}(TMPS)(OH)$. Mixing equally concentrated solutions of $Fe^{III}(TMPS)(OH)$ and sodium cyanide in the volume ratio 1:1 at pH 8 or 9, and 20 °C, resulted in the formation of a small fraction of both monocyano and dicyano species. The spectral changes and stopped-flow kinetic measurements indicated that binding of cyanide to $[Fe^{III}(TMPS)(OH)]$ occurs in two steps.[12,17−20] Under the selected pH conditions the following reactions are to be considered:

$$HCN \rightleftarrows H^+ + CN^- \qquad K_{a(HCN)} \qquad (1)$$

dx.doi.org/10.1021/ic1023345 |*Inorg. Chem.* 2011, 50, 3413–3424

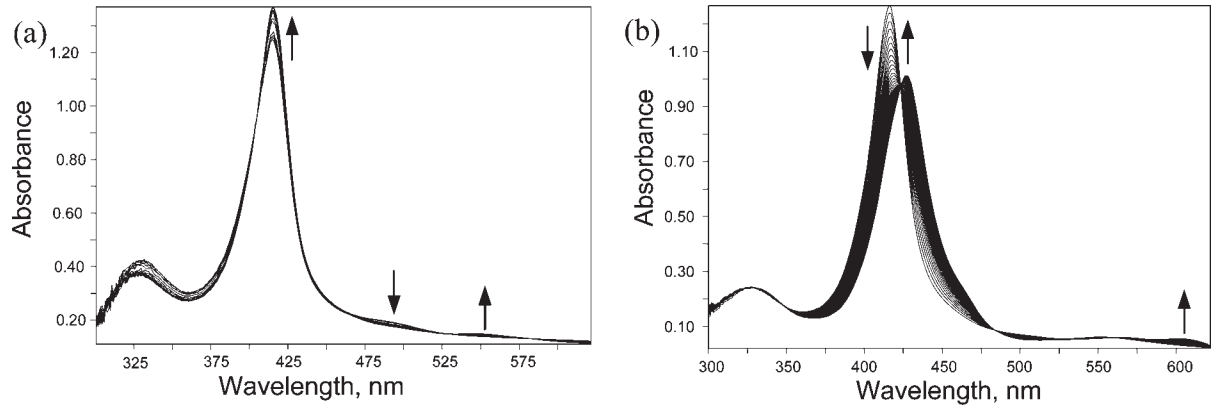

Figure 1. (a) Spectral changes observed during formation of the monocyano porphyrin complex after addition of NaCN to $Fe^{III}(TMPS)(OH)$. Experimental conditions: $[Fe^{III}(TMPS)(OH)] = 1 \times 10^{-5}$ M, $[NaCN] = 1.5 \times 10^{-5}$ M, pH = 8, [TAPS buffer] = 0.05 M, I = 0.15 M ($NaNO_3$). (b) Spectral changes observed during formation of the dicyano porphyrin complex after addition of NaCN to $Fe^{III}(TMPS)(OH)$. Experimental conditions: $[Fe^{III}(TMPS)(OH)] = 1 \times 10^{-5}$ M, $[NaCN] = 5 \times 10^{-4}$ M, pH = 8, [TAPS buffer] = 0.05 M, I = 0.15 M ($NaNO_3$).

$$Fe^{III}(TMPS)(OH) + CN^- \underset{k_{-1}}{\overset{k_1}{\rightleftarrows}} Fe^{III}(TMPS)(CN)(OH)$$
$$K_1 = k_1/k_{-1} \qquad (2)$$

$$Fe^{III}(TMPS)(CN)(OH) + H^+ \rightleftarrows Fe^{III}(TMPS)(CN)(H_2O)$$
$$K_b \qquad (3)$$

$$Fe^{III}(TMPS)(CN)(H_2O) + CN^- \underset{k_{-2}}{\overset{k_2}{\rightleftarrows}} Fe^{III}(TMPS)(CN)_2 + H_2O$$
$$K_2 = k_2/k_{-2} \qquad (4)$$

The coordination of cyanide to $Fe^{III}(TMPS)(OH)$ in the first step leads to the formation of the six-coordinate species $Fe^{III}(TMPS)(CN)(OH)$ (reaction 2). The strong labilizing effect of CN^- is expected to increase the pK_a value of coordinated H_2O, on which basis we suggest that under the studied pH conditions, rapid protonation of OH^- follows the first cyanide binding (reaction 3). Such a conclusion is in line with literature data which show that the presence of an anionic ligand like OH^- or CN^- in the trans position strongly increases the pK_a value of coordinated water up to ≈11−12 in comparison with that for the diaqua-ligated form.[20,21] In the next step binding of a second cyanide ion leads to the formation of the six-coordinate $Fe^{III}(TMPS)(CN)_2$ species. The stopped-flow kinetic measurements for cyanide binding to $Fe^{III}(TMPS)(OH)$ at pH 8 and 20 °C were carried out under pseudo-first-order conditions, and revealed a linear dependence of $k_{obs(n)}$ on $[CN^-]$ (representing the concentration of free cyanide at a particular pH) (eq 5) for reactions 2 and 4 (Figure 2). It is important to note that Figure 2 refers to the free cyanide concentration (eq 6) on the abscissa, and the pseudo-first-order kinetic conditions are fulfilled by the presence of an appropriate large pool of nondissociated HCN in solution (p$K_{a(HCN)}$ = 9.2 at 20 °C).

$$k_{obs(n)} = k_n[CN^-] + k_{-n} \qquad n = 1, 2 \qquad (5)$$

where

$$[CN^-] = \left(\frac{K_{a(HCN)}}{[H]^+ + K_{a(HCN)}}\right)[NaCN] \qquad (6)$$

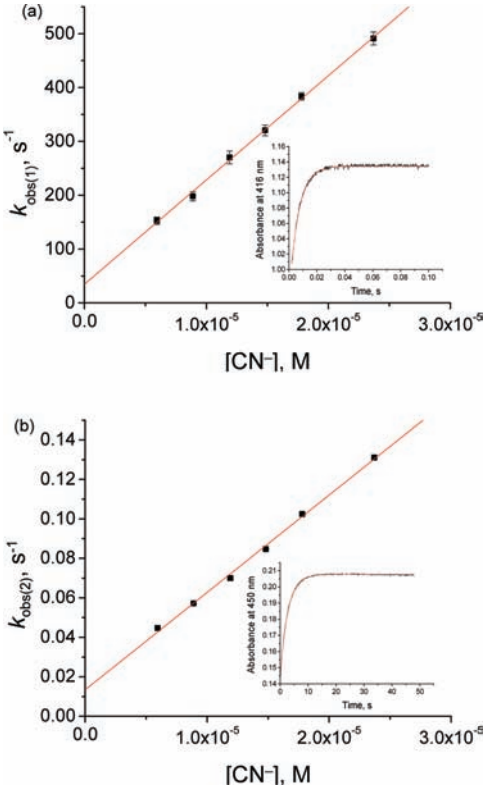

Figure 2. Dependence of $k_{obs(n)}$ on $[CN^-]$ for the reaction of CN^- with $Fe^{III}(TMPS)(OH)$ at pH 8: (a) binding of first CN^- to $Fe^{III}(TMPS)(OH)$, inset: typical kinetic trace at λ = 416 nm, $[CN^-] = 5.9 \times 10^{-6}$ M; (b) binding of second CN^- to $Fe^{III}(TMPS)(CN)(H_2O)$, inset: typical kinetic trace at λ = 450 nm, $[CN^-] = 5.9 \times 10^{-6}$ M. Experimental conditions: $[Fe^{III}(TMPS)(OH)] = 1 \times 10^{-5}$ M, pH = 8, [TAPS buffer] = 0.05 M, I = 0.15 M ($NaNO_3$), T = 20 °C.

Since the ratio of the rate constants for reactions 2 and 4 at pH 8 is sufficiently large ($k_1/k_2 \approx 4 \times 10^3$), the observed rate constants, $k_{obs(1)}$ and $k_{obs(2)}$ were determined independently by fitting a single exponential function to the recorded kinetic traces. Taking into account that formation of $Fe^{III}(TMPS)(CN)_2$ is preceded by protonation of $Fe^{III}(TMPS)(CN)(OH)$

dx.doi.org/10.1021/ic1023345 |Inorg. Chem. 2011, 50, 3413–3424

Table 1. Rate and Equilibrium Constants for the Reversible Binding of Cyanide to Fe^{III}(TMPS)(OH) and Fe^{III}(TMPS)(CN)(H_2O) at pH 8 and 9, and 20 °C

	pH = 8	pH = 9
k_1 [M^{-1} s^{-1}]	$(1.92 \pm 0.04) \times 10^7$	
k_{-1} [s^{-1}]	35 ± 6	
k_2 [M^{-1} s^{-1}]	$(4.9 \pm 0.1) \times 10^3$	$(4.8 \pm 0.1) \times 10^3$
k_{-2} [s^{-1}]	$(1.3 \pm 0.2) \times 10^{-2}$	
k''_{-2} [s^{-1}][a]	$(1.54 \pm 0.01) \times 10^{-2}$	$(1.66 \pm 0.01) \times 10^{-2}$
K_1 [M^{-1}]	$(5.5 \pm 0.9) \times 10^5$	
K_2 [M^{-1}]	$(3.8 \pm 0.6) \times 10^5$	
K''_2 [M^{-1}][a]	$(3.2 \pm 0.1) \times 10^5$	$(3.2 \pm 0.4) \times 10^5$

[a] k''_{-2} represents k_{-2} obtained from the reaction of Fe^{III}(TMPS)$(CN)_2$ with NO; K''_2 represents the equilibrium constant calculated using k''_{-2}.

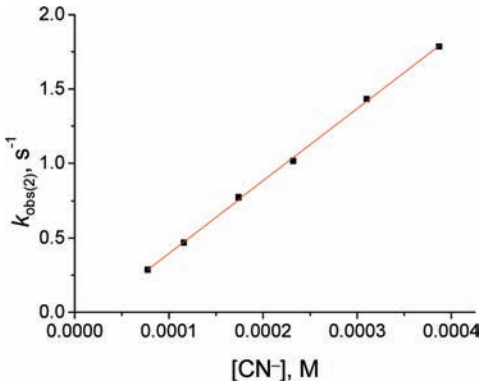

Figure 3. Dependence of $k_{obs(2)}$ on [CN^-] for the reaction of CN^- with Fe^{III}(TMPS)(CN)(H_2O), reaction 4 at pH 9. Experimental conditions: [Fe^{III}(TMPS)(OH)] = 1×10^{-5} M, [CHES buffer] = 0.05 M, I = 0.15 M ($NaNO_3$), 20 °C, λ = 455 nm.

to form Fe^{III}(TMPS)(CN)(H_2O), the observed rate constant $k_{obs(2)}$ can be expressed as in eq 7.

$$k_{obs(2)}^{pH8} = \frac{k_2 K_b [CN^-][H^+]}{1 + K_b[H^+]} + k_{-2} \qquad (7)$$

It is reasonable to assume that at pH 8, $K_b[H^+] \gg 1$ and eq 7 reduces to eq 5. The insets of Figures 2a and 2b present typical kinetic traces recorded for reactions 2 and 4 at pH 8 at 416 and 450 nm, respectively. The rate constants for cyanide binding (k_n) and release (k_{-n}) calculated from the slope and intercept of these plots, respectively, are summarized in Table 1.

Formation of the monocyano derivative at pH 9 was found to be too fast to be measured by stopped-flow technique. Therefore, kinetic measurements were performed only for reaction 4 under such conditions. The observed rate constants were determined by fitting a single exponential function to the kinetic traces. A plot of the resulting $k_{obs(2)}$ values versus the cyanide concentration was found to be linear over the selected [CN^-] range (Figure 3), but the extrapolation of $k_{obs(2)}$ to [CN^-] = 0 did not give an intercept that could be used to determine k_{-2}.

On the basis that the formation of Fe^{III}(TMPS)(CN)(OH) occurs in a fast pre-equilibrium step, which is followed by fast protonation to form Fe^{III}(TMPS)(CN)(H_2O) and the second cyanide binding reaction, the observed rate constant can be expressed as in eq 8. Since the dependence of $k_{obs(2)}$ on [CN^-] at pH 9 is linear, it can be concluded that under the applied conditions $K_1K_b[H^+][CN^-] \gg 1 + K_1[CN^-]$, such that eq 8 can be simplified to the linear form expressed as in eq 5. However, this simplification is only true at appropriately high [CN^-] since at lower [CN^-] a curved dependence of $k_{obs(2)}$ on [CN^-] will be observed. Therefore, the square dependence of the observed rate constant on the cyanide concentration expressed by eq 8 accounts for our inability to determine k_{-2} after simplification of this equation to the linear expression 5.

$$k_{obs(2)}^{pH9} = \frac{k_2 K_1 K_b [H^+][CN^-]^2}{1 + K_1[CN^-] + K_1K_b[H^+][CN^-]} + k_{-2} \qquad (8)$$

The rate constant for the release of cyanide from Fe^{III}(TMPS)$(CN)_2$ was also determined in the reaction of Fe^{III}(TMPS)$(CN)_2$ with NO (denoted as k''_{-2}) at both pH values, which gave more accurate values of k_{-2} (see section on "Kinetic studies on the reaction of NO with Fe^{III}(TMPS)$(CN)_2$") (Table 1). The general agreement observed for the data at pH 8 and 9 in Table 1 indicates that a correct model was used to fit these data to obtain pH independent parameters. The independence of the rate constants k_2 and k''_{-2} on pH substantiates our assumption that at both studied pH values the major species that undergoes a reaction with CN^- is Fe^{III}(TMPS)(CN)(H_2O). If the second axial ligand in the monocyano derivative was OH^-, a dependence of the rate constant for binding of the second CN^- on pH would be observed.

The pK_a value of Fe^{III}(TMPS)$(H_2O)_2$ is 6.9 and thus at pH 8 only about 7% of the porphyrin complex exists in the diaqua-ligated form.[6] Unfortunately, the pK_a value for the Fe^{III}(TMPS)(CN)(H_2O) intermediate is presently unknown. Determination of the pK_a value for the latter species was not possible since its formation could not be observed at higher pH. We assume that the pK_a value for Fe^{III}(TMPS)(CN)(H_2O) is $\geq$11, in agreement with the value of 12.2 reported for Fe^{III}(TMPyP)(CN)(H_2O).[20] Therefore, it is reasonable to conclude that the binding of CN^- to the five-coordinate Fe^{III}(TMPS)(OH) species leads to a considerable decrease in the pK_b value, and thus rapid protonation leads to the monoaquamonocyano complex. Furthermore, it is well-known that coordination of two negatively charged ligands like OH^- or CH_3O^- to the relatively electron-rich iron center in Fe^{III}(TMPS) is not observed even at a high nucleophile concentration, unless it is CN^-. Therefore, the formation of Fe^{III}(TMPS)(CN)(OH) is highly unlikely in the studied pH range.[6,22]

Comparison of the second order rate constant $k_1 = (1.92 \pm 0.04) \times 10^7$ M^{-1} s^{-1} for reaction 2 determined at pH 8, with the rate constants for the reaction of cyanide with met-myoglobin and met-hemoglobin, namely, $(2-5) \times 10^2$ M^{-1} s^{-1} at pH $\approx$ 7 and 20 °C, and 3×10^2 M^{-1} s^{-1} at pH 9.2 and 20 °C, respectively,[23−26] shows that the reaction with hemoproteins occurs almost 5 orders of magnitude slower than with the Fe^{III}(TMPS)(OH) complex and seems not to depend on the nature of the binding species, namely, HCN or CN^-. There are three key factors which cannot be ignored when differences between cyanide binding to model porphyrins and hemoproteins are discussed: (i) the protein environment which regulates ligand movement into the distal pocket, (ii) HCN deprotonation, and (iii) dissociation of coordinated water. A detailed study of various myoglobin mutants showed that in the case of HCN binding, ligand diffusion into the protein is not the rate-determining

dx.doi.org/10.1021/ic1023345 |Inorg. Chem. 2011, 50, 3413–3424

step.[25,26] The major factor that controls cyanide binding to the protein heme center is deprotonation of HCN, which depends on the polarity of the distal pocket and its accessibility to solvent.[25,26] In contrast to that, it has been reported that binding of the anion N_3^- is mainly governed by its accessibility to the heme site.[25] It seems likely that also in the case of CN^-, ligand movement into the distal pocket is the dominant barrier. Furthermore, under the studied conditions, CN^- binding to Fe(TMPS)(OH) does not require displacement of a solvent molecule since the sixth coordination site is vacant in Fe^{III}(TMPS)(OH). In met-myglobin or met-hemoglobin the sixth coordination site is occupied and the dissociation of a water molecule is required. Therefore, the strength of solvent coordination seems to be crucial. In the case of ligand coordination to the iron center that is not preceded by deprotonation at physiological pH, for example, N_3^-, it has been shown that the absence of water in the sixth coordination position entails a significant increase in the binding rate constant.[25,27]

The ratio of the rate constants k_n/k_{-n} gave the equilibrium constants $K_1 = (5.5 \pm 0.9) \times 10^5\ M^{-1}$ and $K_2 = (3.8 \pm 0.6) \times 10^5\ M^{-1}$ for reactions 2 and 4, respectively at pH 8. Despite the small value of k_2 in comparison to k_1, K_2 is relatively high, which is due to a much smaller rate constant for cyanide release from the dicyano than from the monocyano complex. At pH 8, the equilibrium constant K_2 calculated using the k_{-2} value obtained from the intercept is within the error limits in good agreement with the K''_2 value calculated by using k''_{-2} obtained from the reaction with NO (see further Discussion).

Unfortunately, the determination of activation parameters for reaction 2 was not possible because of the high rate of the reaction and the limitations of the instrumentation to follow such reactions as a function of temperature and pressure. Therefore, kinetic measurements as a function of temperature and pressure were performed only for the formation of Fe^{III}(TMPS)$(CN)_2$ at pH 8 and 9. In all the calculations of reaction and activation parameters, the concentration of free cyanide was used and calculated by taking the dependence of $K_{a(HCN)}$ on temperature and pressure into account.[28,29] In addition, the influence of temperature and pressure on the pH of the employed buffers was also considered.[30−32] The rate constants for CN^- binding (k_2) in the temperature range from 15 to 40 °C enabled to construct an Eyring plot (Figure 4a) and to calculate $\Delta H^{\ddagger}_2$ and $\Delta S^{\ddagger}_2$ from the slope and intercept, respectively.

In addition, the effect of pressure on the kinetics of the reaction of Fe^{III}(TMPS)(CN)(H_2O) with cyanide was studied over the pressure range 10−130 MPa. Plots of $\ln(k_2)$ versus pressure were found to be linear and enabled to determine the volume of activation ($\Delta V^{\ddagger}_2$) (Figure 4b). Pressure experiments were repeated at least two times, and the reported $\Delta V^{\ddagger}_2$ values were calculated as the mean value. At the applied concentration of cyanide the contribution of k_{-2} to $k_{obs(2)}$ can be neglected and then $k_{obs(2)} = k_2[CN^-]$. The activation parameters for the binding of cyanide to Fe^{III}(TMPS)(CN)(H_2O), determined at pH 8 and 9, are summarized in Table 2. The activation parameters for release of CN^- from Fe^{III}(TMPS)$(CN)_2$ were determined in a more direct way, namely, in the reaction with NO (see section on "Kinetic studies on the reaction of NO with Fe^{III}(TMPS)$(CN)_2$") and are included in Table 2.

To determine the standard reaction parameters for reaction 4, UV−vis spectra were monitored as a function of temperature and pressure in the presence of 30- and 15-fold excess of NaCN over the porphyrin complex at pH 8 and 9, respectively. The relatively high excess of total cyanide used and the clean isosbestic points observed over the applied temperature and pressure ranges confirmed that the observed spectral changes can be exclusively attributed to reaction 4. The thermodynamic equilibrium constants (K^{th}_2) at 20 °C were found to be in good agreement at both studied pHs, namely, 2.7×10^5 and $1.9 \times 10^5\ M^{-1}$, and correlate very well with the kinetically determined values (see Tables 1 and 2).

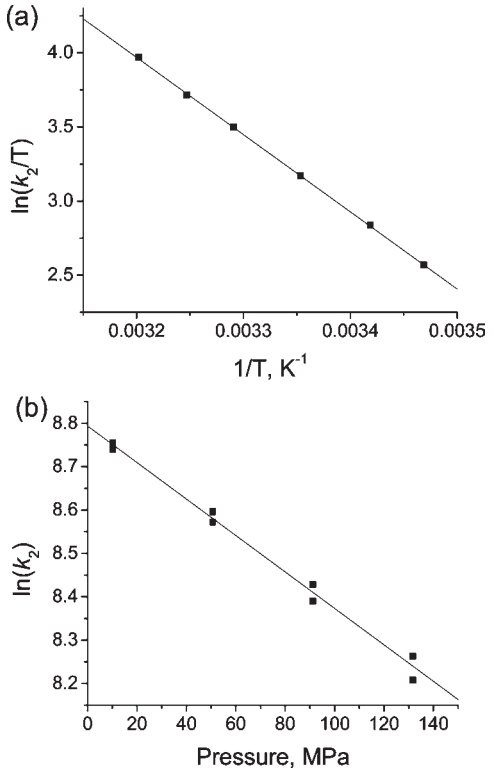

Figure 4. Temperature and pressure dependence for the binding of CN^- to Fe^{III}(TMPS)(CN)(H_2O). (a) Eyring plot of $\ln(k_2/T)$ vs $1/T$ (b) plot of $\ln(k_2)$ vs pressure, T = 25 °C. Experimental conditions: [Fe^{III}(TMPS)(OH)] = 1×10^{-5} M, [NaCN] = 8×10^{-4} M, pH = 8, [TAPS buffer] = 0.05 M, I = 0.15 M ($NaNO_3$), λ = 450 nm. To calculate k_2, the concentration of free cyanide was used and changes in $pK_{a(HCN)}$ with temperature and pressure, as well as changes in the pH of the buffers with temperature were taken into account.

The influence of temperature on the equilibrium constant (K^{th}_2) was monitored over the temperature range from 10 to 40 °C. The increase in temperature caused a shift in equilibrium (4) toward the reactants (Figure 5a). The values of $\ln(K^{th}_2)$ obtained over the selected temperature range show a linear dependence on $1/T$ (Figure 5a, inset) and enabled to determine $\Delta H°$ and $\Delta S°$ from the slope and intercept, respectively. High pressure experiments were performed at 30 °C over the pressure range from 5 to 150 MPa. The observed spectral changes were completely reversible and indicated that increasing pressure shifted equilibrium (4) toward the product side (Figure 5b). A plot of $\ln(K^{th}_2)$ versus pressure showed a linear dependence (Figure 5b, inset), and the value of the slope was used to calculate $\Delta V°$. All calculated thermodynamic parameters for the reaction of Fe^{III}(TMPS)(CN)(H_2O) with cyanide are included in Table 2.

dx.doi.org/10.1021/ic1023345 |*Inorg. Chem.* 2011, 50, 3413–3424

Table 2. Summary of Reaction and Activation Parameters for the Reversible Binding of CN^- to $Fe^{III}(TMPS)(CN)(H_2O)$ at pH 8 and 9[a]

	pH = 8		pH = 9	
kinetic and thermodynamic parameters	CN^- binding $\Delta X^{\ddagger}_2$	CN^- release $\Delta X^{\ddagger}_{-2}$[b]	CN^- binding $\Delta X^{\ddagger}_2$	CN^- release $\Delta X^{\ddagger}_{-2}$[b]
$\Delta H^{\ddagger}$ (kJ mol^{-1})	43.3 ± 0.3	92 ± 1	37 ± 1	94 ± 3
$\Delta S^{\ddagger}$ (J mol^{-1} K^{-1})	−26 ± 1	+36 ± 2	−50 ± 3	+41 ± 9
$\Delta V^{\ddagger}$ (cm^3 mol^{-1})	+10.4 ± 0.4	+11.2 ± 0.3	+13 ± 1	+15 ± 1
K^{th}_2 (M^{-1}) at 20 °C	2.7×10^5		1.9×10^5	
$\Delta H°$ (kJ mol^{-1})	−54.6 ± 0.2		−61 ± 1	
$\Delta S°$ (J mol^{-1} K^{-1})	−82 ± 1		−107 ± 5	
$\Delta V°$ (cm^3 mol^{-1})	−3.9 ± 0.4		−5.0 ± 0.2	

[a] X represents H, S, V, respectively. [b] Activation parameters determined through the reaction of $Fe^{III}(TMPS)(CN)_2$ with NO.

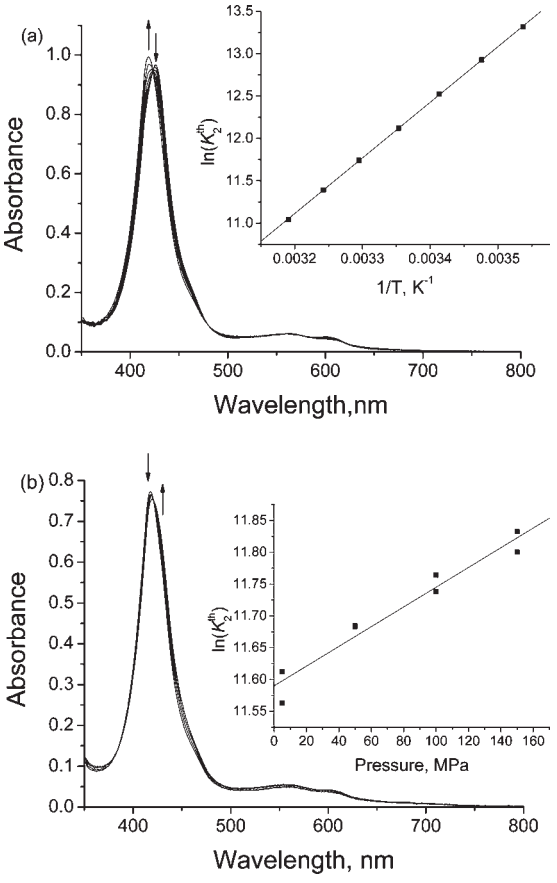

Figure 5. (a) Temperature induced spectral changes for reaction 4, inset: plot of $\ln(K^{th}_2)$ vs $1/T$. Experimental conditions: $[Fe^{III}(TMPS)(OH)] = 1 \times 10^{-5}$ M, $[NaCN] = 3 \times 10^{-4}$ M, pH = 8, [TAPS buffer] = 0.05 M, I = 0.15 M ($NaNO_3$), P = 0.1 MPa; (b) Pressure induced spectral changes, inset: plot of $\ln(K^{th}_2)$ vs pressure. Experimental conditions: $[Fe^{III}(TMPS)(OH)] = 5 \times 10^{-6}$ M, $[NaCN] = 1.5 \times 10^{-4}$ M, pH = 8, [TAPS buffer] = 0.05 M, I = 0.15 M ($NaNO_3$), T = 30 °C. For the calculation of K_2^{th}, the concentration of free cyanide was used, and changes in $pK_{a(HCN)}$ with temperature and pressure, as well as changes in the pH of the buffers with temperature were taken into account.

Mechanism for the Reversible Binding of CN^- to Fe(TMPS)(CN)(H_2O). The positive values of $\Delta V^{\ddagger}$ for the binding and release of the second cyanide ion, confirm the six-coordinate nature of the Fe(TMPS)(CN)(H_2O) complex and suggest a dissociative reaction mechanism. Since coordination of the second CN^- has to be preceded by dissociation of H_2O, the mechanism of the reaction can be expressed by Scheme 1. According to a steady-state approximation on $Fe^{III}(TMPS)(CN)$, the observed first-order rate constant ($k_{obs(2)}$) can be expressed as shown in eq 9.[33]

Scheme 1

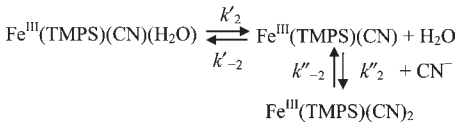

$$k_{obs(2)} = \frac{k'_2 k''_2[CN^-] + k'_{-2}k''_{-2}[H_2O]}{k'_{-2}[H_2O] + k''_2[CN^-]} \quad (9)$$

Under the selected conditions, it can be assumed that $k'_{-2}[H_2O] \gg k''_2[CN^-]$ as no curvature in the dependence of $k_{obs(2)}$ on $[CN^-]$ was observed. Consequently, rate law (9) can be simplified to the expression shown in eq 10, where $k_2 = k'_2 k''_2/k'_{-2}[H_2O]$ and $k_{-2} = k''_{-2}$

$$k_{obs(2)} = \frac{k'_2 k''_2[CN^-]}{k'_{-2}[H_2O]} + k''_{-2} \quad (10)$$

According to eq 10, the activation parameters for the "on" reaction can be expressed as a composite of three terms:

$$\Delta H^{\ddagger}_2 = \Delta H^{\ddagger'}_2 + \Delta H^{\ddagger''}_2 - \Delta H^{\ddagger'}_{-2} \quad (11)$$

$$\Delta S^{\ddagger}_2 = \Delta S^{\ddagger'}_2 + \Delta S^{\ddagger''}_2 - \Delta S^{\ddagger'}_{-2} \quad (12)$$

$$\Delta V^{\ddagger}_2 = \Delta V^{\ddagger'}_2 + \Delta V^{\ddagger''}_2 - \Delta V^{\ddagger'}_{-2} \quad (13)$$

Therefore the values of $\Delta H^{\ddagger}_2$, $\Delta S^{\ddagger}_2$, and $\Delta V^{\ddagger}_2$ for the forward reaction will include compensating effects arising from the different contributions. In terms of $\Delta V^{\ddagger}_2$, the first reaction step in Scheme 1 involves the dissociation of a water molecule for which

dx.doi.org/10.1021/ic1023345 |Inorg. Chem. 2011, 50, 3413–3424

Scheme 2

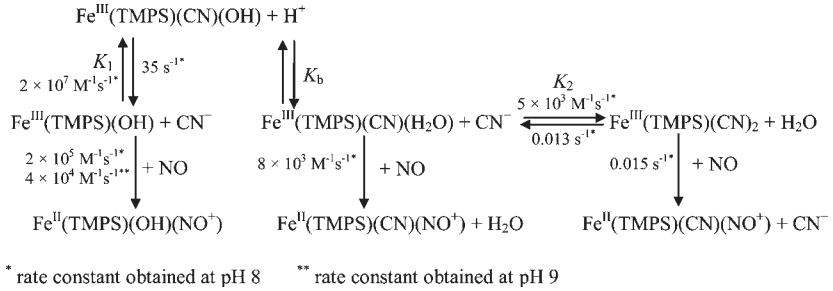

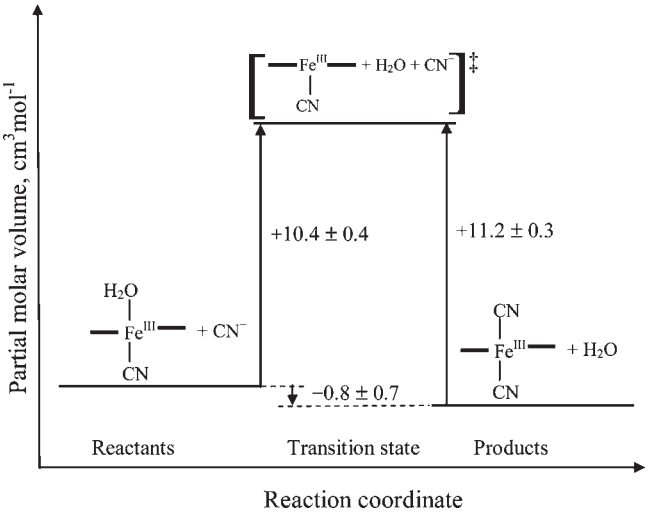

Figure 6. Volume profile for the reversible binding of CN^- to $Fe^{III}(TMPS)(CN)(H_2O)$ according to reaction 4 at pH 8.

$\Delta V^{\ddagger\prime}_2 - \Delta V^{\ddagger\prime}_{-2}$ is expected to be $\sim +13$ cm^3 mol^{-1}, estimated for the release of a water molecule in going from a six- to a five-coordinate complex.[34] This value will be offset by the contribution of $\Delta V^{\ddagger\prime\prime}_2$, expected to be negative for the coordination of cyanide. In many cases the value of $\Delta S^{\ddagger}$ usually reflects the trend in $\Delta V^{\ddagger}$; however, in our case the determined value of $\Delta S^{\ddagger}_2$ was found to be negative, that is, opposite to the positive $\Delta V^{\ddagger}_2$ value. We assume that the obtained value of $\Delta S^{\ddagger}_2$ is a result of the composite nature of k_2. In general, considerable uncertainties contributing to the determination of $\Delta S^{\ddagger}$ limit the usability of this parameter in drawing mechanistic conclusions.

The activation parameters for the release of cyanide (Table 2) are in good agreement at both studied pH values. In accordance with the principle of microscopic reversibility, the "on" and "off" reactions are expected to pass through the same transition state. The positive values of $\Delta S^{\ddagger}_{-2}$ and $\Delta V^{\ddagger}_{-2}$ can be interpreted in terms of a dissociative mechanism in which Fe-CN bond cleavage and changes in electrostriction are responsible for the positive values. The dissociation of CN^- from $[Fe^{III}(TMPS)(CN)_2]^{5-}$ leads to the formation of the five-coordinate intermediate species $[Fe^{III}(TMPS)(CN)]^{4-}$ (see Scheme 1). Although the overall charge does not change on going from products to transition state, charge dilution does take place which can be expected to cause a reduction in the electrostricted water.[35] This in turn will result in a positive contribution to both $\Delta V^{\ddagger}_{-2}$ and $\Delta S^{\ddagger}_{-2}$. On the basis of the reported activation volumes, a volume profile (Figure 6) was constructed for the reversible binding of CN^- to $Fe^{III}(TMPS)(CN)(H_2O)$, which nicely demonstrates the dissociative character of both the forward and the back reactions.

A comparison of the reaction parameters calculated on the basis of kinetic data with those obtained from thermodynamic measurements shows only minor discrepancies. The negative value of $\Delta H°$ demonstrates the exothermic character of reaction 4 that involves the reversible binding of cyanide to $Fe^{III}(TMPS)(CN)(H_2O)$. The reaction entropy and volume values were found to be negative. The overall reaction volume does not only result from the displacement of H_2O by CN^-, but is also due to a change in electrostriction. Charge concentration which occurs on going from $[Fe^{III}(TMPS)(CN)(H_2O)]^{4-}$ to $[Fe^{III}(TMPS)(CN)_2]^{5-}$ (Scheme 1) results in a volume contraction that arises from an increase in electrostriction. Furthermore, a relatively small overall volume collapse confirms the lack of any spin state change on the iron center on going from the low-spin monocyano to the low-spin dicyano complex. As can be expected, the binding of the first cyanide ion to the high-spin, five-coordinate $Fe^{III}(TMPS)(OH)$ complex will involve a change in spin state to form the low-spin $Fe^{III}(TMPS)(CN)(H_2O)$ complex as found for many different six-coordinate mixed-ligand monocyano iron(III) porphyrin species.[10,18]

UV−vis Spectral Data for the Reaction of NO with $Fe^{III}(TMPS)(CN)(H_2O)$ and $Fe^{III}(TMPS)(CN)_2$. As previously mentioned, on mixing cyanide with an aqueous solution of $Fe^{III}(TMPS)(OH)$ at pH 8 and 9 in the concentration ratio 1:1 (or lower) leads to the formation of both $Fe^{III}(TMPS)(CN)(H_2O)$ and $Fe^{III}(TMPS)(CN)_2$. Since the equilibrium constants for reactions 2 and 4 at pH 8 are almost equal (see Table 1), it was not possible to obtain a high yield of the monocyano complex at room temperature. Addition of NO to a deoxygenated solution of $Fe^{III}(TMPS)$ containing a small excess of total cyanide, resulted in spectral changes with no clean isosbestic points that indicated the occurrence of three simultaneous reactions. The fastest reaction leads to the formation of $Fe^{II}(TMPS)(OH)(NO^+)$ with a characteristic Soret band maximum at 430 nm, Q-band at 545 nm and isosbestic points at 420, 447, and 527 nm (Figure 7a). The concurrent slower reaction corresponds to a bathochromic shift of the Soret (434 nm) and Q (553 nm) band maxima, and isosbestic points at 430, 457, and 549 nm. The spectral changes associated with this reaction indicated the formation of $Fe^{II}(TMPS)(CN)(NO^+)$ (Figure 7b). On a much longer time scale, small absorbance changes (no shift in Soret and Q-band, but only absorbance increase) associated with nitrosylation of $Fe^{III}(TMPS)(CN)_2$, were observed. In the presence of a high excess of cyanide, where the main species is $Fe^{III}(TMPS)(CN)_2$,

dx.doi.org/10.1021/ic1023345 |Inorg. Chem. 2011, 50, 3413–3424

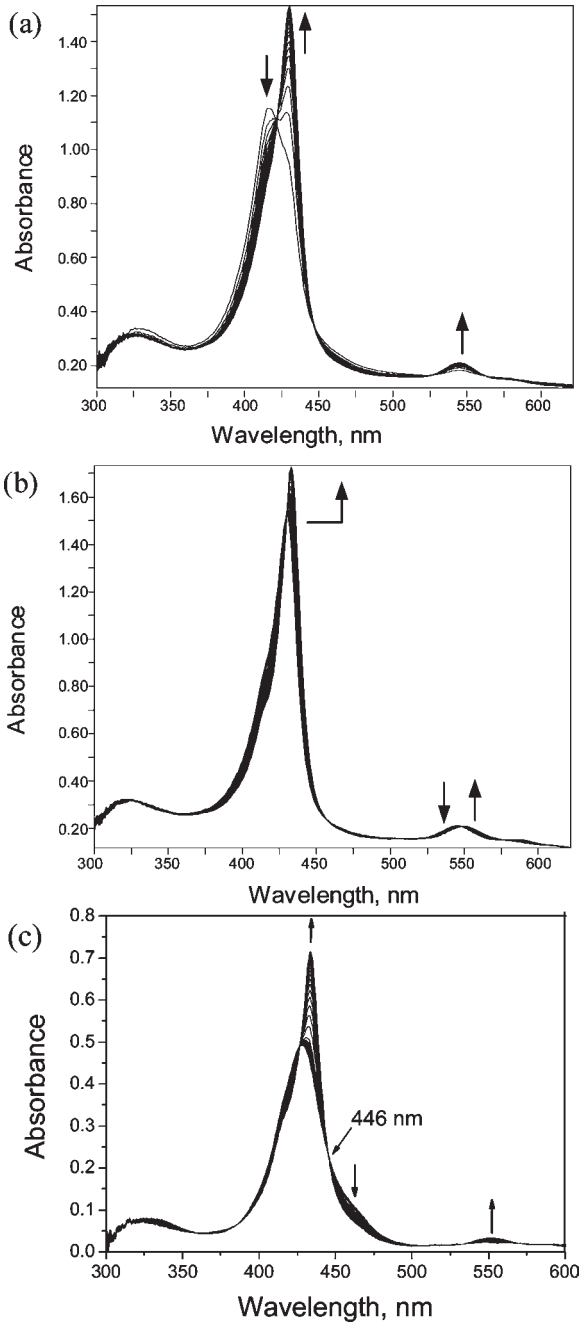

Figure 7. Spectral changes accompanying the nitrosylation of the Fe^{III}(TMPS) complex in the presence of cyanide. (a) Reaction between NO and Fe^{III}(TMPS)(OH) leading to the formation of Fe^{II}(TMPS)(OH)(NO^+), time 0−0.15 s; (b) simultaneous slower reaction between NO and Fe^{III}(TMPS)(CN)(H_2O) leading to the formation of Fe^{II}(TMPS)(CN)(NO^+), time 0.15−20 s. Experimental conditions (a) and (b): [Fe^{III}(TMPS)(OH)] = 1×10^{-5} M, [NaCN] = 2×10^{-5} M, [NO] = 0.9 mM, pH = 8, [TAPS buffer] = 0.05 M, I = 0.15 M ($NaNO_3$), T = 10 °C. (c) Reaction between NO and Fe^{III}(TMPS)$(CN)_2$ leading to the formation of Fe^{II}(TMPS)(CN)(NO^+). Experimental conditions (c): [Fe^{III}(TMPS)(OH)] = 5×10^{-6} M, [NaCN] = 5×10^{-4} M, [NO] = 0.54 mM, pH = 8, [TAPS buffer] = 0.05 M, I = 0.15 M ($NaNO_3$), T = 20 °C.

only one slow reaction was observed after addition of NO. The observed spectral changes with clean isosbestic points (427, 446, and 533 nm) showed a shift of the Soret band to longer wavelength.

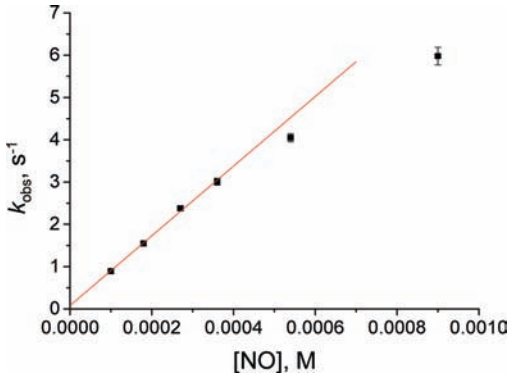

Figure 8. Plot of k_{obs} vs [NO] for the reaction of Fe^{III}(TMPS)(CN)(H_2O) with NO. Experimental conditions: [Fe^{III}(TMPS)(OH)] = 1×10^{-5} M, [NaCN] = 2.5×10^{-4} M, pH = 8, [TAPS buffer] = 0.05 M, I = 0.15 M ($NaNO_3$), λ = 446 nm, T = 20 °C.

New bands appeared at 434 and 553 nm, corresponding to the conversion of Fe^{III}(TMPS)$(CN)_2$ to Fe^{II}(TMPS)(CN)(NO^+) (Figure 7c).

Kinetic Studies on the Reaction of NO with Fe^{III}(TMPS)(CN)(H_2O). The formation of Fe^{II}(TMPS)(CN)(NO^+) was studied under pseudo-first-order conditions by following the reaction of NO with Fe^{III}(TMPS)(CN)(H_2O) in the presence of different concentrations of NaCN and at different temperatures to find the best reaction conditions. Because of the presence of three species in solution, namely, Fe^{III}(TMPS)(OH), Fe^{III}(TMPS)(CN)(H_2O), and Fe^{III}(TMPS)$(CN)_2$, which can simultaneously undergo nitrosylation, the appropriate spectral range had to be selected to monitor the binding of NO to the monocyano complex. The stopped-flow kinetic experiments were performed at 446 nm that corresponds to the isosbestic point for the reaction of NO with Fe^{III}(TMPS)$(CN)_2$ (see Figure 7c) and shows negligible absorbance changes associated with the conversion of Fe^{III}(TMPS)(OH) to Fe^{II}(TMPS)(OH)(NO^+) (see Figure 7a). Furthermore, NO binding to Fe^{III}(TMPS)(CN)(H_2O) was followed in the presence of a relatively large excess of NaCN (1:25) such that the concentration of Fe^{III}(TMPS)(OH) present in solution prior to addition of NO was practically zero. Therefore, at this wavelength only absorbance changes associated with the conversion of Fe^{III}(TMPS)(CN)(H_2O) to Fe^{II}(TMPS)(CN)(NO^+) were observed. The essential advantage of this approach was the possibility to record single exponential kinetic traces,[36] although they were associated with quite small absorbance changes at this wavelength. Furthermore, it is important to note that since the ratio of the observed rate constants for NO binding to Fe^{III}(TMPS)(CN)(H_2O) and Fe^{III}(TMPS)$(CN)_2$ varies from 25 to 267 over the [NO] range from 0.1 to 0.6 mM, respectively, these reactions do not interfere with each other under the selected reaction conditions (see Figures 8 and 9). The data in Figure 8 show that the observed rate constants increase linearly with [NO] at low NO concentration and display a slight saturation at higher NO concentrations. The latter is ascribed to complications arising from side reactions that occur under these conditions.

The second-order rate constant calculated from the data in the lower NO concentration range by fitting a linear dependence to the data presented in Figure 8 has a value of $(8.2 \pm 0.3) \times 10^3\ M^{-1}\ s^{-1}$. It is important to note that the observed rate constants depend on the cyanide concentration present in solution, that is, with

dx.doi.org/10.1021/ic1023345 |*Inorg. Chem.* 2011, 50, 3413–3424

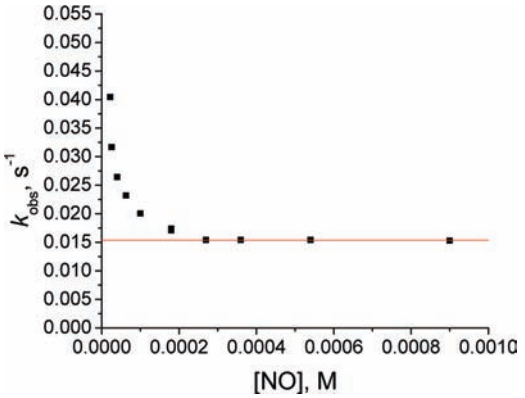

Figure 9. Dependence of k_{obs} on the NO concentration. Experimental conditions: $[Fe^{III}(TMPS)(OH)] = 5 \times 10^{-6}$ M, [NaCN] = 5×10^{-4} M, pH = 8, [TAPS buffer] = 0.05 M, I = 0.15 M ($NaNO_3$), λ = 460 nm, T = 20 °C.

increasing excess of [NaCN] k_{obs} also increases. Accordingly, determination of an accurate value of the second order rate constant for NO binding to $Fe^{III}(TMPS)(CN)(H_2O)$ was impossible (it is in the order of 10^3 M^{-1} s^{-1} at 20 °C for concentration ratios of $[Fe^{III}(TMPS)(OH)]$ to [NaCN] from 1:1 to 1:25). This indicates that equilibrium 2 does contribute to the observed rate constant. The presence of three different complexes in solution that simultaneously, but at different rate constants, bind NO, made it very difficult to follow the nitrosylation of only the monocyano complex. Scheme 2 summarizes the three reactions which lead to two different nitrosyl complexes, as well as the concomitant equilibria between the reactant species.

The data at 20 °C presented in Scheme 2 indicate that the estimated rate constant for NO binding to $Fe^{III}(TMPS)(CN)(H_2O)$ is lower than the rate constant for NO binding to $Fe^{III}(TMPS)(OH)$. This can be ascribed to dissociation of the aqua ligand which has to precede NO binding to $Fe^{III}(TMPS)(CN)(H_2O)$, leading to the formation of $Fe^{II}(TMPS)(CN)(NO^+)$. Furthermore, the rate constant for cyanide release from the monocyano complex is relatively high. Therefore, it can be expected that for the applied [NO] range the monohydroxo nitrosyl complex, $Fe^{II}(TMPS)(OH)(NO^+)$, is produced in a relatively high quantity, even though only traces of $Fe^{III}(TMPS)(OH)$ are present in solution prior to the addition of NO. This conclusion is supported by the fact that nitrosylation of $Fe^{III}(TMPS)(OH)$ was observed even if the ratio of the $Fe^{III}(TMPS)(OH)$ complex to cyanide concentration was very high, namely, 1:25. The presence of such a large excess of cyanide will lead to the existence of mainly the dicyano species and only a small fraction of the monocyano species, which was confirmed by spectra recorded after mixing $Fe^{III}(TMPS)(OH)$ with cyanide in the concentration ratio 1:25.

Taking into account that the binding of NO has to be preceded by the dissociation of one axial ligand, the mechanism of the reaction can be presented by Scheme 3. Accordingly, the monocyano species reacts with NO along two parallel pathways leading to two different reaction products as described above.

The major reaction pathway proceeds through the dissociation of water, followed by the binding of NO to the five-coordinate monocyano complex to produce $Fe^{II}(TMPS)(CN)(NO^+)$. The second pathway involves deprotonation of coordinated water,

Scheme 3

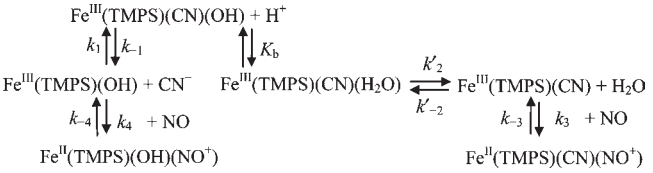

Scheme 4

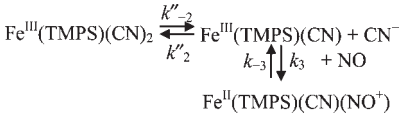

followed by dissociation of CN^-. In the next step rapid NO binding to the five-coordinate monohydroxo complex leads to formation of $Fe^{II}(TMPS)(OH)(NO^+)$.

Kinetic Studies on the Reaction of NO with $Fe^{III}(TMPS)(CN)_2$. Kinetic studies on the binding of NO to $Fe^{III}(TMPS)(CN)_2$ were performed in the presence of a high excess of NaCN to eliminate other possible side reactions. The binding of NO to $Fe^{III}(TMPS)(CN)_2$ is described by reaction 14.

$$Fe^{III}(TMPS)(CN)_2 + NO \underset{k_{off}}{\overset{k_{on}}{\rightleftharpoons}} Fe^{II}(TMPS)(CN)(NO^+) + CN^- \quad (14)$$

Single exponential kinetic traces were recorded at 460 nm and 20 °C. The observed rate constants decreased with increasing [NO] to reach a limiting value at high [NO] (Figure 9). Such a correlation between k_{obs} and [NO] can be attributed to the operation of a limiting dissociative mechanism as depicted in Scheme 4. By applying a steady-state approximation to the five-coordinate intermediate $Fe^{III}(TMPS)(CN)$, the observed first-order rate constant can be expressed as in eq 15.[33]

$$k_{obs} = \frac{k''_{-2}k_3[NO] + k''_2k_{-3}[CN^-]}{k''_2[CN^-] + k_3[NO]} \quad (15)$$

The characteristic decrease in k_{obs} with increasing [NO], is a consequence of the smaller value of k''_{-2} in comparison to k_{-3}. Nevertheless, at a high [NO] the observed rate constant shows no dependence on the NO concentration, which can be accounted for in terms of a limiting dissociative mechanism in which the release of CN^- from $Fe^{III}(TMPS)(CN)_2$ is the rate-determining step of the reaction. Therefore, eq 15 can be reduced to $k_{obs} = k_{on} = k''_{-2}$. Thus, the values of k_{on}, namely, $(1.54 \pm 0.01) \times 10^{-2}$ and $(1.66 \pm 0.01) \times 10^{-2}$ s^{-1} at pH 8 and 9, respectively, were calculated using NO concentrations in the range from 0.27 to 0.9 mM. These results suggest that the first-order rate constant for the nitrosylation of $Fe^{III}(TMPS)(CN)_2$ corresponds to the first-order rate constant for the dissociation of CN^-, that is, $k_{on} = k_{-2}$. Therefore, the reaction of NO with $Fe^{III}(TMPS)(CN)_2$ can be used to determine the value of k_{-2} more accurately, since the determination of k_{-2} from the intercept was coupled to large uncertainties (see Table 1). The upper limit of k_{-3} is ≤ 0.1 s^{-1} (see Figure 9) and much slower than the release of NO by $Fe^{II}(TMPS)(OH)(NO^+)$ (k_{-4}),[6]

dx.doi.org/10.1021/ic1023345 |Inorg. Chem. 2011, 50, 3413–3424

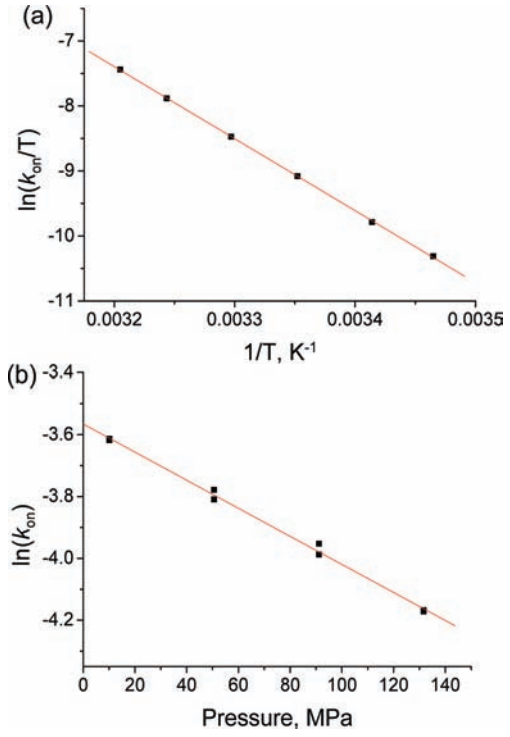

Figure 10. Temperature and pressure dependence for the binding of NO to $Fe^{III}(TMPS)(CN)_2$. (a) Eyring plot of $\ln(k_{on}/T)$ vs $1/T$. (b) Plot of $\ln(k_{on})$ vs pressure, T = 25 °C. Experimental conditions: $[Fe^{III}(TMPS)(OH)]$ = 7.5 × 10^{-6} M, [NaCN] = 5.6 × 10^{-4} M, [NO] = 0.9 mM, pH = 8, [TAPS buffer] = 0.05 M, I = 0.15 M ($NaNO_3$), λ = 455 nm.

which indicates that OH^- has a stronger labilizing effect than CN^- in the present system.

For more detailed information on the binding mechanism of NO to $Fe^{III}(TMPS)(CN)_2$, the temperature dependence of k_{obs} was measured over the range 15 to 40 °C under limiting [NO] conditions. At both selected pH values, plots of $\ln(k_{on}/T)$ correlated linearly with $1/T$ (Figure 10a). The values of the activation enthalpy ($\Delta H_{on}^{\ddagger}$) (pH 8: 92.0 ± 0.6 kJ mol^{-1}; pH 9: 94 ± 3 kJ mol^{-1}) and activation entropy ($\Delta S_{on}^{\ddagger}$) (pH 8: +36 ± 2 J mol^{-1} K^{-1}; pH 9: +41 ± 9 J mol^{-1} K^{-1}) are in good agreement within the error limits at both pH values. Further insight into the reaction mechanism was obtained by applying high pressure (10−130 MPa) kinetic measurements, which indicated positive activation volumes, namely, +11.2 ± 0.3 and +15.3 ± 0.5 cm^3 mol^{-1} at pH 8 and pH 9, respectively. The linear dependence of $\ln(k_{on})$ on pressure used to determine $\Delta V_{on}^{\ddagger}$, is presented in Figure 10b.

The positive values of the activation parameters $\Delta S_{on}^{\ddagger}$ and $\Delta V_{on}^{\ddagger}$ reported for the binding of NO to $Fe^{III}(TMPS)(CN)_2$ are consistent with a limiting dissociative mechanism in which Fe^{III}−CN bond cleavage is the rate-determining step. We were not able to determine the activation parameters for the release of NO from $Fe^{II}(TMPS)(CN)(NO^+)$, but on the basis of microscopic reversibility we suggest that the reverse reaction passes through the same five-coordinate intermediate as shown in Scheme 4. Therefore, it is reasonable to expect that the back reaction follows the same limiting dissociative substitution mechanism. As mentioned above, according to the limiting dissociative mode of NO binding to $Fe^{III}(TMPS)(CN)_2$, the activation parameters for the "on" reaction with NO are synonymous with those for cyanide release from $Fe^{III}(TMPS)(CN)_2$. Therefore, the activation parameters $\Delta H^{\ddagger}_{-2} = \Delta H^{\ddagger}_{on}$, $\Delta S^{\ddagger}_{-2} = \Delta S^{\ddagger}_{on}$, and $\Delta V^{\ddagger}_{-2} = \Delta V^{\ddagger}_{on}$ summarized in Table 2, were obtained from the nitrosylation of $Fe^{III}(TMPS)(CN)_2$ as described above.

A similar limiting dissociative mechanism was proposed for the nitrosylation of $Fe^{III}(TMPS)(OH)(MeIm)$ in the ionic liquid [emim][NTf_2], 1-ethyl-3-methylimidazolium bis-trifluoromethylsulfonylamide, where the formation of the six-coordinate $Fe^{III}(TMPS)(OH)(MeIm)$ complex was connected with the presence of methylimidazole impurities at a micromolar level in the ionic liquid.[8] The kinetic data showed an independence of k_{obs} on [NO], suggesting that the release of methylimidazole is the rate-determining step of the reaction rather than the binding of NO. The first-order rate constant, k_{on} = (7.0 ± 0.2) × 10^{-2} s^{-1} found for the nitrosylation of $Fe^{III}(TMPS)(OH)(MeIm)$ is comparable with that obtained for the reaction of NO with $Fe^{III}(TMPS)(CN)_2$. On the contrary, NO binding to the five-coordinate $Fe^{III}(TMPS)(OH)$ complex in basic aqueous solution follows an associative mechanism.[6] The obtained results indicate that the presence of a strong ligand in the sixth axial position strongly affects NO coordination to the metal center and results in a changeover in the nitrosylation mechanism. Earlier conclusions drawn from studies on water-soluble iron(III) porphyrins and ferriheme proteins confirm that NO binding could be mainly governed by axial ligand lability.[2,3(c)] However, the influence of an overall spin transition and related structural changes can play a crucial role in the reactivity of NO toward ferriporphyrins.[6] The ability of NO to substitute CN^- in $Fe^{III}(TMPS)(CN)_2$ suggests a very high affinity of this signaling molecule for the iron(III) center. Colman and co-workers previously reported that NO can substitute inhibitors of cytochrome *c* oxidase like CN^- and CO, and so act as "antidote" for their poisoning.[37] Taking advantage of the fact that cyanide dissociation is the rate-determining step in the nitrosylation of cyanide ligated myoglobin, the k_{off} rate constant for cyanide release from ferric myoglobin was found to be 4.3 × 10^{-4} s^{-1}.[23] This value is more than a 100 times smaller than the value found in this study for the release of cyanide from $Fe^{III}(TMPS)(CN)_2$.

CONCLUSIONS

The reported study revealed detailed insight into the mechanism of the reactions of CN^- with the water-soluble ferric porphyrin, $Fe^{III}(TMPS)$. The obtained kinetic and thermodynamic data for CN^- coordination to the Fe(III) center provide a better understanding of the mechanism of nitric oxide binding to the cyano complexes $Fe^{III}(TMPS)(CN)(H_2O)$ and $Fe^{III}(TMPS)(CN)_2$. The positive activation volume and independence of the rate constant on pH for the binding of the second cyanide ion to the monocyano species imply the six-coordinate nature of the complex and presence of a water ligand in the axial position trans to cyanide. Nitrosylation of both $Fe^{III}(TMPS)(CN)(H_2O)$ and $Fe^{III}(TMPS)(CN)_2$ resulted in the formation of the same species, namely, $Fe^{II}(TMPS)(CN)(NO^+)$. Detailed kinetic studies on the coordination of NO to $Fe^{III}(TMPS)(CN)_2$ indicated that nitrosylation occurs via a limiting dissociative mechanism.

The obtained results allow us to draw a conclusion related to the effect of the axial ligands on the reactivity pattern of NO with ferriporphyrins. The presence of a strong nucleophile in the sixth

axial position results in a changeover of the mechanism of NO binding to the iron(III) center in comparison with the mechanism observed for nitrosylation of five-coordinate porphyrin complexes. Furthermore, the fact that NO is able to substitute the CN^- ligand in $Fe^{III}(TMPS)(CN)_2$, further supports that NO can be a better ligand than cyanide also in iron(III) hemoproteins. Accordingly, the mechanism of CN^- substitution by NO proposed in the present study can shed more light on the mechanism of the recovery process in the treatment of cyanide inhibition of cytochrome *c* oxidase.

AUTHOR INFORMATION

Corresponding Authors

*E-mail: vaneldik@chemie.uni-erlangen.de (R.v.E.), stochel@chemia.uj.edu.pl (G.S.).

ACKNOWLEDGMENT

This work was supported by the International Ph.D. Study Program at the Faculty of Chemistry, Jagiellonian University, within the Foundation for Polish Science MPD Program cofinanced by the European Regional Development Fund. The research was carried out with equipment purchased with financial support from the European Regional Development Fund within the framework of the Polish Innovation Economy Operational Program (contract no. POIG.02.01.00-12-023/08). A.F. and R.v.E. gratefully acknowledge continued financial support from the Deutsche Forschungsgemeinschaft.

REFERENCES

(1) (a) Koshland, D. E. *Science* **1992**, *258*, 1861–1865. (b) Culotta, E.; Koshland, D. E. *Science* **1992**, *258*, 1862–1865.

(2) (a) Ford, P. C.; Lorkovic, I. M. *Chem. Rev.* **2002**, *102*, 993−118 and references therein. (b) Laverman, L. E.; Ford, P. C. *J. Am. Chem. Soc.* **2001**, *123*, 11614−11622 and references therein. (c) Ford, P. C.; Laverman, L. E.; Lorkovic, I. M. *Adv. Inorg. Chem.* **2003**, *54*, 203–257 and references therein.

(3) (a) Franke, A.; Stochel, G.; Jung, C.; van Eldik, R. *J. Am. Chem. Soc.* **2004**, *126*, 4181−4191 and references therein. (b) Theodoridis, A.; van Eldik, R. *J. Mol. Catal. A: Chem.* **2004**, *224*, 197–205. (c) Hoshino, M.; Ozawa, K.; Seki, H.; Ford, P. C. *J. Am. Chem. Soc.* **1993**, *115*, 9568–9575. (d) Hoshino, M.; Kogure, M. *J. Phys. Chem.* **1989**, *93*, 5478–5484. (e) Wanat, A.; Wolak, M.; Orzel, L.; Brindell, M.; van Eldik, R.; Stochel, G. *Coord. Chem. Rev.* **2002**, *229*, 37–49.

(4) Laverman, L. E.; Wanat, A.; Oszajca, J.; Stochel, G.; Ford, P. C.; van Eldik, R. *J. Am. Chem. Soc.* **2001**, *123*, 285–293.

(5) (a) Jee, J.-E.; Eigler, S.; Jux, N.; Zahl, A.; van Eldik, R. *Inorg. Chem.* **2007**, *46*, 3336–3352. (b) Jee, J.-E.; Wolak, M.; Balbinot, D.; Jux, N.; Zahl, A.; van Eldik, R. *Inorg. Chem.* **2006**, *45*, 1326–1337. (c) Jee, J.-E.; Eigler, S.; Hampel, F.; Jux, N.; Wolak, M.; Zahl, A.; Stochel, G.; van Eldik, R. *Inorg. Chem.* **2005**, *44*, 7717–7731.

(6) Wolak, M.; van Eldik, R. *J. Am. Chem. Soc.* **2005**, *127* 13312–13315.

(7) Franke, A.; Roncaroli, F.; van Eldik, R. *Eur. J. Inorg. Chem.* **2007**, *6*, 773−798 and references therein.

(8) Schmeisser, M.; van Eldik, R. *Inorg. Chem.* **2009**, *48*, 7466–7475.

(9) (a) Ikezaki, A.; Ikeue, T.; Nakamura, M. *Inorg. Chim. Acta* **2002**, *335*, 91–99. (b) Nakamura, M.; Ikeue, T.; Ikezaki, A.; Ohgo, Y.; Fujii, H. *Inorg. Chem.* **1999**, *38*, 3857–3862. (c) Nakamura, M.; Ikeue, T.; Fujii, H.; Yoshimura, T. *J. Am. Chem. Soc.* **1997**, *119*, 6284–6291.

(10) Li, J.; Noll, B. C.; Schulz, C. E.; Scheidt, W. E. *Inorg. Chem.* **2007**, *46*, 2286–2298.

(11) (a) Patra, R.; Rath, S. P. *Inorg. Chem. Commun.* **2009**, *12*, 515–519. (b) Bartczak, T. J.; Wolowiec, S.; Latos-Grazynski, L. *Inorg. Chim. Acta* **1998**, *277*, 242–246. (c) Balch, A. L.; Noll, B. C.; Safari, N. *Inorg. Chem.* **1993**, *32*, 2901–2905. (d) Schappacher, M.; Fischer, J.; Weiss, R. *Inorg. Chem.* **1989**, *28*, 389–390. (e) Hada, M. *J. Am. Chem. Soc.* **2004**, *126*, 486–487. (f) Ikezaki, A.; Nakamura, M. *Inorg. Chem.* **2002**, *41*, 2761–2768.

(12) Scheidt, W. R.; Haller, K. J.; Hatano, K. *J. Am. Chem. Soc.* **1980**, *102*, 3017–3021.

(13) (a) Stochel, G. *Coord. Chem. Rev.* **1992**, *114*, 269–295. (b) Stasicka, Z.; Wasielewska, E. *Coord. Chem. Rev.* **1997**, *159*, 271–294. (c) Oszajca, J.; Stochel, G.; Wasielewska, E.; Stasicka, Z.; Gryglewski, R. J.; Jakubowski, A.; Cieslik, K. *J. Inorg. Biochem.* **1998**, *69*, 121–127.

(14) (a) Beasley, D. M.; Glass, W. I. *Occup. Med. (Lond.)* **1998**, *48*, 427–431. (b) Cumings, T. F. *Occup. Med. (Lond.)* **2004**, *54*, 82–85. (c) Brenner, M.; Mahon, S. B.; Lee, J.; Kim, J.; Mukai, D.; Goodman, S.; Kreuter, K. A.; Ahdout, R.; Mohammad, O.; Sharma, V. S.; Blackledge, W.; Boss, G. R. *J. Biomed. Opt.* **2010**, *15*, 017001. (d) Broderick, K. E.; Potluri, P.; Zhuang, S.; Scheffler, I. E.; Sharma, V. S.; Pilz, R. B.; Boss, G. R. *Exp. Biol. Med. (Maywood, NJ, U. S.)* **2006**, *231*, 641–649. (e) Bhattacharya, R.; Tulsawani, R. *J. Environ. Biol.* **2009**, *30*, 515–520.

(15) (a) van Eldik, R.; Palmer, D. A.; Schmidt, R.; Kelm, H. *Inorg. Chim. Acta* **1981**, *50*, 131–135. (b) van Eldik, R.; Gaede, W.; Wieland, S.; Kraft, J.; Spitzer, M.; Palmer, D. A. *Rev. Sci. Instrum.* **1993**, *64*, 1355–1357.

(16) Spitzer, M.; Garting, F.; van Eldik, R. *Rev. Sci. Instrum.* **1988**, *59*, 2092–2093.

(17) Silver, J.; Taies, J. A. *Inorg. Chim. Acta* **1989**, *159*, 231–235.

(18) Wang, J.-T.; Yeh, H. J. C.; Johnson, D. F. *J. Am. Chem. Soc.* **1978**, *100*, 2400–2405.

(19) Goff, H.; Morgan, L. O. *Inorg. Chem.* **1976**, *15*, 2069–2076.

(20) Arifuku, F.; Ujimoto, K.; Kurihara, H. *Bull. Chem. Soc. Jpn.* **1986**, *59*, 149–154.

(21) (a) Kobayashi, N. *Inorg. Chem.* **1985**, *24*, 3324–3330. (b) Kobayashi, N.; Koshiyama, N.; Osa, T.; Kuwana, T. *Inorg. Chem.* **1983**, *22*, 3608–3614.

(22) Wolak, M.; van Eldik, R. *Chem.—Eur. J.* **2007**, *13*, 4873–4883.

(23) Ascenzi, P.; di Masi, A.; Gullotta, F.; Mattu, M.; Ciaccio, C.; Coletta, M. *Biochem. Biophys. Res. Commun.* **2010**, *393*, 196−200 and references therein.

(24) Sybert, D. W.; Mofat, K.; Gibson, Q. H. *J. Biol. Chem.* **1976**, *251*, 45–52.

(25) Brancaccio, A.; Cutruzzolz, F.; Allocatelli, C. T.; Brunori, M.; Smerdon, S. J.; Wilkinson, A. J.; Dou, Y.; Keenan, D.; Ikeda-Saito, M.; Brantley, R. E.; Olson, J. S. *J. Biol. Chem.* **1994**, *35*, 13843–13853.

(26) Dou, Y.; Olson, J. S.; Wilkinson, A. J.; Ikeda-Saito, M. *Biochemistry* **1996**, *35*, 7107–7113.

(27) (a) Giacometti, G. M.; Da Ros, A.; Antonini, A.; Brunori, M. *Biochemistry* **1975**, *14*, 1584–1585. (b) Giacometti, G. M.; Ascenzi, P.; Bolognesi, M.; Brunori, M. *J. Mol. Biol.* **1981**, *146*, 363–374. (c) Bolognesi, M.; Coda, A.; Frigerio, F.; Gatti, G.; Ascenzi, P.; Brunori, M. *J. Mol. Biol.* **1991**, *213*, 621–625. (d) Mattevi, A.; Gatti, G.; Coda, A.; Rizzi, M.; Ascenzi, P.; Brunori, M.; Bolognesi, M. *J. Mol. Recognit.* **1991**, *4*, 1–6.

(28) Marques, H. M.; Brown, K. L.; Jacobsen, D. W. *J. Biol. Chem.* **1988**, *263*, 12378–12383.

(29) Lambier, A. M.; Heremans, K.; Dunford, H. B. *Biophys. Chem.* **1983**, *18*, 195–201.

(30) Kitamura, Y.; Ioth, T. *J. Solution Chem.* **1987**, *16*, 715–725.

(31) Goldberg, R. N.; Kishore, N.; Lennen, R. *J. Phys. Chem. Ref. Data* **2002**, *31*, 231–370.

(32) By using the concentration of free cyanide to calculate the reaction and activation parameters for reaction 4 makes them independent of the ionization of HCN (ΔH_{HCN} = 45 kJ mol^{-1}, ΔS_{HCN} = −22 J mol^{-1} K^{-1} and ΔV_{HCN} = −6.5 cm^3 mol^{-1}). Since $[CN^-]$ depends on $[H^+]$ (eq 6), changes in pH with temperature and pressure were taken into account. According to the thermodynamic data for the ionization of the buffers, namely, TAPS (ΔH = 40 kJ mol^{-1}, ΔS = −26 J mol^{-1} K^{-1} and ΔV = 0.5 cm^3 mol^{-1}) and CHES (ΔH = 39 kJ mol^{-1}, ΔS = −47 J mol^{-1} K^{-1} and ΔV = 1 cm^3 mol^{-1}), the $[H^+]$ calculated at particular temperatures were used to calculate $[CN^-]$, whereas changes in pH with pressure

were negligible since the values of ΔV for the ionization of the buffers are very small.

(33) Malin, J. M.; Toma, H. E.; Giesbrecht, E. *J. Chem. Educ.* **1977**, *54*, 385–386.

(34) Swaddle, T. W. *Adv. Inorg. Bioinorg. Mechanisms*; Academic Press Inc.: New York, 1983; Vol. 2, p 95.

(35) van Eldik, R.; Asano, T.; le Noble, W. J. *Chem. Rev.* **1989**, *89*, 549–688.

(36) Espenson, J. H. *Chemical Kinetics and Reaction Mechanisms*, 2nd ed.; McGraw-Hill, Inc.: New York, 1995; 3.6 and 4.1, pp 62−64 and 75.

(37) Colman, J. P.; Dey, A.; Decreau, R. A.; Yang, Y.; Hosseini, A.; Solomon, E. I.; Eberspacher, T. A. *Proc. Natl. Acad. Sci. U.S.A.* **2008**, *105*, 9892–9896.